Report

The *NEMO* Mutation Creating the Most-Upstream Premature Stop Codon Is Hypomorphic Because of a Reinitiation of Translation

Anne Puel,[1,*] Janine Reichenbach,[1,*,†] Jacinta Bustamante,[1] Cheng-Lung Ku,[1] Jacqueline Feinberg,[1] Rainer Döffinger,[1,‡] Marion Bonnet,[1,§] Orchidée Filipe-Santos,[1] Ludovic de Beaucoudrey,[1] Anne Durandy,[2] Gerd Horneff,[6,‖] Francesco Novelli,[1,¶] Volker Wahn,[6,#] Asma Smahi,[3] Alain Israel,[5] Tim Niehues,[6] and Jean-Laurent Casanova[1,4]

[1]Laboratoire de Génétique Humaine des Maladies Infectieuses, INSERM U550, Faculté de Médecine Necker-Enfants Malades, [2]Développement Normal et Pathologique du Système Immunitaire, INSERM U429, [3]Unité de Recherches sur les Handicaps Génétiques de l'Enfant, INSERM U393, and [4]Unité d'Immunologie et d'Hématologie Pédiatriques, Hôpital Necker-Enfants Malades, and [5]Unité de Signalisation Moléculaire et Activation Cellulaire, URA 2582 Centre National de la Recherche Scientifique, Institut Pasteur, Paris; and [6]Pädiatrische Immunologie und Rheumatologie, Zentrum für Kinderheilkunde, Heinrich Heine Universität, Düsseldorf, Germany

Amorphic mutations in the NF-κB essential modulator (NEMO) cause X-dominant incontinentia pigmenti, which is lethal in males in utero, whereas hypomorphic mutations cause X-recessive anhidrotic ectodermal dysplasia with immunodeficiency, a complex developmental disorder and life-threatening primary immunodeficiency. We characterized the *NEMO* mutation *110_111insC*, which creates the most-upstream premature translation termination codon (at codon position 49) of any known *NEMO* mutation. Surprisingly, this mutation is associated with a pure immunodeficiency. We solve this paradox by showing that a Kozakian methionine codon located immediately downstream from the insertion allows the reinitiation of translation. The residual production of an NH_2-truncated NEMO protein was sufficient for normal fetal development and for the subsequent normal development of skin appendages but was insufficient for the development of protective immune responses.

The human *IKBKG* locus is located on chromosome Xq28 and encodes NEMO. Amorphic *NEMO* mutations are associated with a complete lack of NF-κB activation via the classical pathway. They are responsible for incontinentia pigmenti (IP), an X-linked dominant disorder that is lethal in hemizygous males in utero and is characterized by abnormalities in ectoderm-derived tissues, including the skin, eyes, CNS, and teeth, in heterozygous females. About 85% of patients with IP who have *NEMO* mutations carry a complex rearrangement of the *NEMO* gene that results in a frameshift deletion of exons 4–10 and encodes a putative truncated protein consisting of the first 133 N-terminal amino acids. A number of other IP-causing mutations have been identified in exons 2–10, including mutations associated with premature stop codons (Smahi et al. 2000; Aradhya et al. 2001*b*; Fusco et al. 2004). Blood leukocytes and fibroblasts expressing the mutated X-chromosome are selectively eliminated around the time of birth, leading to skewed X-inactivation in female carriers (Parrish et al. 1996).

Other *NEMO* mutations are hypomorphic, since they

Received October 3, 2005; accepted for publication January 13, 2006; electronically published February 15, 2006.

Address for correspondence and reprints: Dr. Jean-Laurent Casanova, Laboratoire de Génétique Humaine des Maladies Infectieuses, Université de Paris René Descartes-INSERM U550, Faculté de Médecine Necker-Enfants Malades, 156 Rue de Vaugirard, 75015 Paris, France. E-mail: casanova@necker.fr

* Both of these authors contributed equally to this work.

† Present affiliation: Zentrum der Kinderheilkunde und Jugendmedizin, Klinikum der Johann Wolfgang Goethe-Universität, Frankfurt, Germany.

‡ Present affiliation: Department of Clinical Biochemistry and Immunology, Addenbrookes Hospital, Cambridge, United Kingdom.

§ Present affiliation: Department of Pathology, New York University School of Medicine, New York.

‖ Present affiliation: Department of Pediatrics, Asklepios Clinic Sankt Augustin, Sankt Augustin, Germany.

¶ Present affiliation: Centro Oncologico Ematologico Subalpino, Centro Ricerche Medicina Sperimentale, Ospedale San Giovanni Battista, Torino, Italy.

Present affiliation: Immunodeficiency Center of the Charité, Department of Pediatric Pulmonology and Immunology, Humboldt University, Berlin.

Am. J. Hum. Genet. 2006;78:691–701. 0002-9297/2006/7804-0015$15.00

impair but do not abolish NF-κB activation via the classical pathway. They are associated with two closely related but distinct X-recessive (XR) forms of anhidrotic ectodermal dysplasia (EDA) with immunodeficiency (ID). A mutation of the stop codon (X420W) results in the more severe syndrome of osteopetrosis (O), lymphoedema (L), and EDA-ID (XR-OL-EDA-ID) (Smahi et al. 2000; Döffinger et al. 2001; Mansour et al. 2001; Dupuis-Girod et al. 2002). Most of the other mutations, including a few mutations creating premature stop codons, cause XR-EDA-ID without OL (Abinun et al. 1996; Zonana et al. 2000; Aradhya et al. 2001*a*; Döffinger et al. 2001; Jain et al. 2001; Kosaki et al. 2001; Mansour et al. 2001; Dupuis-Girod et al. 2002; Orange et al. 2002; Carrol et al. 2003; Jain et al. 2004; Nishikomori et al. 2004; Orange et al. 2004*a*, 2004*b*; Puel et al. 2004; Ku et al. 2005*a*, 2005*b*). The clinical features of EDA typically include the poor development of skin appendages, resulting in hypo- or anhidrosis with dry skin and heat intolerance; hypo- or atrichosis with sparse hair, eyebrows, and eyelashes; and hypo- or anodontia with conical incisors (Priolo and Lagana 2001; Ku et al. 2005*a*).

Patients with XR-EDA-ID suffer less from developmental defects than from severe infections, most of which are caused by pyogenic bacteria and mycobacteria (Abinun et al. 1996; Smahi et al. 2000; Zonana et al. 2000; Aradhya et al. 2001*a*; Döffinger et al. 2001; Jain et al. 2001; Dupuis-Girod et al. 2002; Orange et al. 2002, 2004*a*; Carrol et al. 2003; Niehues et al. 2004; Nishikomori et al. 2004; Ku et al. 2005*a*). In a few cases, infections with fungi (Zonana et al. 2000; Döffinger et al. 2001; Dupuis-Girod et al. 2002; Orange et al. 2004*a*) and viruses (Döffinger et al. 2001; Orange et al. 2002, 2004*a*) have been documented. Almost half the known patients with XR-EDA-ID died of infection. The most consistent immunological abnormality found in these patients is a poor serum-antibody response to polysaccharide antigens (reviewed by Puel et al. [2004]; Ku et al. [2005*b*]). Two unrelated patients bearing mutations in *NEMO,* with pure IDs and no apparent developmental defect—ID without EDA—were recently described (Niehues et al. 2004; Orange et al. 2004*b*). The first patient carries a splice mutation *1056(−1)G→A* (Orange et al. 2004*b*), which results in the skipping of exon 9, with a premature stop codon inserted at position 373. We report here the characterization of the *110_111insC* mutation in exon 2 in the second patient (Niehues et al. 2004).

The patient's clinical features have been reported in detail elsewhere (Niehues et al. 2004). This patient, a boy, was the only child of healthy nonrelated Polish parents living in Germany. From the age of 15 mo, he suffered from multiple episodes of disseminated *Mycobacterium avium* disease (affecting mostly lymph nodes and bones). At the age of 7 years, he was diagnosed with bronchiectasis caused by *Haemophilus influenzae* and *Streptococcus pneumoniae*. At the age of 11 years, the patient presented extra-intestinal disease caused by *Salmonella enteritidis*. He presented severe autoimmune hemolytic anemia at the age of 12 years and died from herpes simplex virus 1 (HSV-1) meningo-encephalitis at the age of 12 years and 10 mo.

The immunological work-up of this patient, from the age of 2 years, showed low IgA and IgG levels, with markedly high serum IgM levels. No serum antibodies against diphtheria toxoid and tetanus toxoid were detected, and titers of antibodies against *H. influenzae* were low despite complete routine vaccination. The patient also presented low serum titers of antibodies against *S. pneumoniae* and had no allo-hemagglutinin antibodies. Known molecular causes of hyper IgM syndrome, including defects in CD40, CD154, and activation-induced cytidine deaminase, were excluded. Because of the patient's low serum IgG levels, prophylactic intravenous immunoglobulin replacement therapy was initiated at 2 years of age and continued until his death. The numbers of T, B, and NK lymphocytes and the proportions of the $CD4^+$ and $CD8^+$ T lymphocyte subsets were within normal ranges at the ages of 2 and 4 years. However, the patient lacked memory B cells, since all his B cells had the naive IgD^+CD27^- phenotype. The proliferative responses of T lymphocytes to mitogens (PHA and PWM) were normal.

Genomic DNA was isolated from whole blood cells, granulocytes, SV40-transformed fibroblasts, and Epstein Barr virus (EBV)–transformed B cells by a standard phenol/chloroform extraction method. Total RNA was isolated from SV40-transformed fibroblasts by use of Trizol (GibcoBRL Life Technologies, Invitrogen SARL). Both cDNA and individual *IKBKG* exons were amplified using specific primers (primers and conditions for PCR amplification and sequencing are available on request), were sequenced using the Big Dye Terminator cycle sequencing kit (Applied Biosystems), and were analyzed on an ABI Prism 3700 apparatus (Applied Biosystems).

The X-chromosome inactivation status was evaluated by the analysis of DNA methylation at the human androgen receptor gene (*HUMARA*), as described elsewhere (Allen et al. 1992). In brief, genomic DNA (200 ng) extracted from whole blood was digested with 10 IU of *Hpa*II (Invitrogen SARL) at 37°C overnight, in 50 μl of final reaction mixture. After digestion, the reaction was stopped by incubation of the mixture at 95°C for 6 min. A mock sample as control was prepared simultaneously without the *Hpa*II. Twenty-five microliters of each digested product was then used in a 50-μl PCR containing 200 μM of dinucleotide triphosphate (Invitrogen SARL), 1 IU of *Taq* polymerase (AmpliTaq; Applied Biosystems), 1.5 mM of $MgCl_2$, 50 mM of KCl,

10 mM of Tris-HCl (pH 8.3), and 20 μM of each primer. The primers used were AR-F 5′-GCTGTGAAGGTTGCGTTCCTCAT-3′ and AR-R 5′-TCCAGAATCTGTTCCAGAGCGTGC-3′; the AR-F was fluorescent. After an initial denaturation step at 95°C, samples were amplified for 30 cycles (1 min at 94°C, 1 min at 62°C, and 1 min at 72°C), with a final extension step for 10 min. Two microliters of PCR products (mock and *Hpa*II) were then added to a mixture containing 10 μl of deionized formamide and 0.1 μl molecular weight standard GENESCAN 400HD (ROX). The samples were denatured for 6 min at 95°C, were cooled on ice, and were resolved using the 3100 ABI Prism Genetic Analyzer (Applied Biosystems). The percentage of inactivation was calculated as reported elsewhere (Chitnis et al. 2000).

Total or nuclear cell extracts were prepared from SV40-transformed fibroblasts or 293T HEK cells left unstimulated or stimulated with TNF-α (20 ng/ml; R&D Systems Europe) or IL-1β (20 ng/ml; R&D Systems Europe). Electrophoresis, western blot, and electrophoretic mobility shift assay (EMSA) were performed as described elsewhere (Döffinger et al. 2001; Picard et al. 2003). The rabbit anti-human IKKα (H-744, sc-7218), mouse anti-human IKKβ (H-4, sc-8014), mouse anti-human STAT-2 (A-7, sc-1668), rabbit anti-mouse p38 (C-20, sc-535), mouse anti-human IKKγ (B-3, sc-8032), goat anti-human IKKγ (M-18, sc-8256), and rabbit anti-human IκBα (C-21, sc-37) antibodies were purchased from SantaCruz Biotechnology (Tebu-Bio S.A.). The mouse anti-human IKKγ/NEMO (611306) was purchased from BD Transduction Laboratories (Becton Dickinson France S.A.S.), the mouse anti-human IKKγ/NEMO (557383) was purchased from BD Pharmingen (Becton Dickinson France S.A.S.), the rabbit anti-human IKKγ/NEMO (3328) and anti-IκBε (1775) antibodies were kindly provided by G. Courtois and A. Israel, and the mouse anti-V5 monoclonal antibody (5960-25) was purchased from Invitrogen (Invitrogen SARL). The EMSA was performed by incubating 10 μg of nuclear extract with a ^{32}P-labeled double-stranded NF-κB–specific oligonucleotide κB probe (5′-GATCATGGGGAATCCCCA-3′ and 5′-GATCTGGGGATTCCCCAT-3′). Supershift experiments were performed with goat anti-human p50 (C-19, sc-1190) and rabbit anti-human p65 (C-20, sc-372) antibodies from Santa Cruz Biotechnology (Tebu-Bio S.A.).

Cytokine production was assessed in whole blood diluted 1:2 in RPMI 1640 (GibcoBRL Life Technologies) and activated with TNF-α (20 ng/ml; R&D Systems Europe), IL-12p70 (20 ng/ml; R&D Systems Europe), IL-1β (20 ng/ml; R&D Systems Europe), IL-18 (50 ng/ml; R&D Systems Europe), and IL-12 plus IL-18 or phorbol 12-myristate 13-acetate (PMA) plus ionomycin (10^{-7} M and 10^{-5} M, respectively) (Sigma-Aldrich Chimie SARL) for 48 h. For toll-like receptor (TLR)–agonist activation, whole blood diluted 1:5 in RPMI 1640 (GibcoBRL) was incubated with polymyxin B (10 μg/ml; Sigma-Aldrich) (except for stimulation by gram-negative bacteria and lipopolysaccharide [LPS]) at 37°C for 30 min. Cells were then activated with TLR ligands: PAM_3CSK_4 (100 ng/ml; EMC Microcollections), which mimics gram-negative bacteria, recognized by TLR1 and TLR2; PAM_2CSK_4 (100 ng/ml; EMC Microcollections), which mimics gram-positive *Mycoplasma* lipoprotein; zymosan A from yeast (125 μg/ml; Molecular Probes, Invitrogen SARL) and peptidoglycan from *Staphylococcus aureus* (30 μg/ml; Sigma-Aldrich), recognized by TLR2 and TLR6; lipoteichoic acid from *S. aureus* (50 μg/ml; Sigma-Aldrich), recognized by TLR2; poly(I:C) double-stranded RNA (50 μg/ml; Sigma-Aldrich), which mimics RNA viruses, recognized by TLR3; LPS from *Salmonella minnesota* R595 (10 μg/ml; Sigma-Aldrich), recognized by TLR4; flagellin from the flagellated gram-negative bacterium *Salmonella typhimurium* (10 ng/ml; provided by K. D. Smith, Institute for Systems Biology), recognized by TLR5; imidazoquinoline 3M-13, recognized by TLR7 (provided by 3M Pharmaceuticals and 3M Innovative Properties); and CpG oligonucleotide DNA (5′-TCGTCGTTTTGTCGTTTTGTCGTT-3′) (20 μg/ml; Research Genetics, Invitrogen SARL), recognized by TLR9. Several TLR agonists were kindly provided by Adrian Ozinsky. Whole bacteria were also used: heat-killed *S. aureus* (5×10^6 particles/ml; ATCC, LGC Promochem), *Escherichia coli* (5×10^6 particles/ml; ATCC), and H37Rv strain of *Mycobacterium tuberculosis* (*M. tb*) (1 μg/ml; provided by J. Belisle, TB Research Materials and Vaccine Testing Contract, NIH, NIAID NO1 AI-75320). For Bacille Calmette-Guérin (BCG) activation, whole blood was diluted 1:2 in RPMI 1640 (GibcoBRL Life Technologies) and was incubated for 12 or 48 h with live BCG (*Mycobacterium bovis* BCG, Pasteur substrain) at a multiplicity of infection of 20:1, BCG plus IFN-γ (5,000 IU/mL), and BCG plus recombinant IL-12p70 (20 ng/ml; R&D Systems Europe). Supernatants were collected after 12 or 48 h, and the secretion of IL-12p40, IFNγ, IL-6, IL-10, and TNF-α was measured using human IL-12p40 (R&D Systems Europe), IFNγ, IL-6, IL-10, and TNF-α (Sanquin, Mast Diagnostic) ELISA kits, respectively, in accordance with the manufacturer's instructions. For SV40-transformed fibroblast activation, cells were activated by incubation for 18 h with TNF-α or IL-1β (10 ng/ml; R&D Systems Europe), and IL-6 production was measured by ELISA (Sanquin, Mast Diagnostic). In vitro B-cell proliferation was measured in peripheral blood lymphocytes stimulated by incubation for 5 d with sCD154 (1 μg/ml; Amgen France), by the addition of ^{3}H-thymidine for the final 18 h (1 μCi). IgE production was measured by ELISA in the supernatants of peripheral blood lympho-

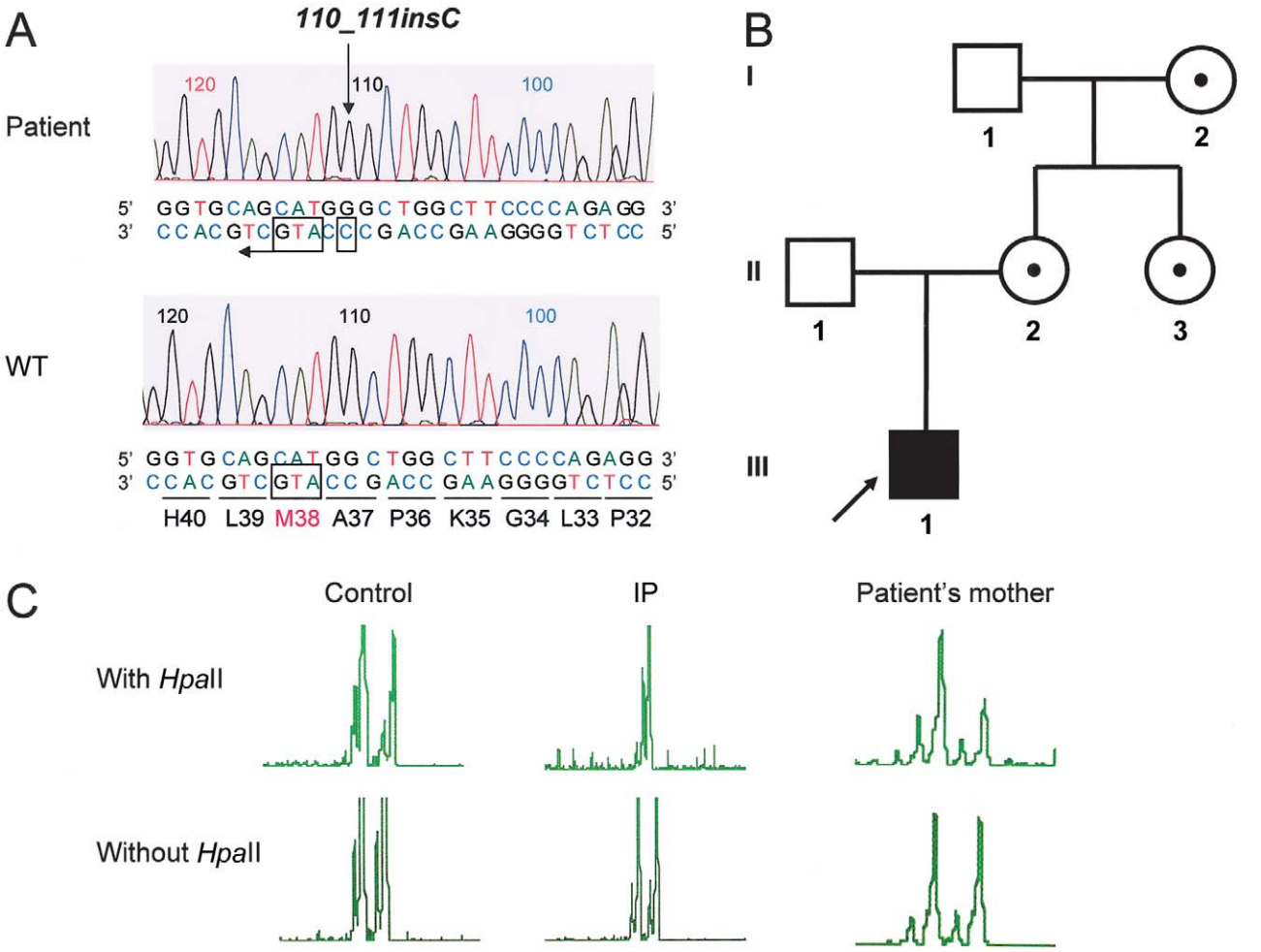

Figure 1 Sequencing of the *NEMO* gene in the patient and his relatives. *A*, Automated reverse-sequencing profile showing the *110_111insC* mutation in genomic DNA extracted from peripheral blood cells from the hemizygous patient, compared with a control (WT) with the corresponding amino-acid sequence, and the M38 reinitiation site (*boxed*). *B*, Pedigree of the family. Each generation is designated by a roman numeral (I–III) and each individual is designated by an arabic numeral (1–3); the hemizygous patient is shown in black. Heterozygous carriers are shown with a black dot in the center. *C*, X-inactivation pattern in blood cells from a healthy female control, from a female patient with IP carrying the common IP *NEMO ex4_10del* mutation, and from the patient's mother.

cytes stimulated for 12 d with sCD154 plus IL-4 (100 U/ml; R&D Systems Europe).

The full-length human *IKBKG* cDNA, inserted between the *Hin*dIII and *Not*I sites of the expression vector pcDNA3, was a gift from G. Courtois. We generated various *IKBKG* mutations, using the QuikChange Site-Directed Mutagenesis kit (Stratagene) in accordance with the manufacturer's procedure. The patient's *110_111insC* mutation was generated using the primers P-CCTCTGGGGAAGCCAGCCCATGCTGCACCTGCCTTC and P-GAAGGCAGGTGCAGCATGGGCTGGCTTCCCCAGAGG, the IP mutation R62X using the primers P-GAGAATCAAGAGCTCTGAGATGCCATCCGGCAG and P-CTGCCGGATGGCATCTCAGAGCTCTTGATTCTC, the XL-OL-EDA-ID mutation X420W using the primers P-CATGGAGTGCATTGAGTGGGGCCGGCCAGTGCAAGG and P-CCTTGCACTGGCCGGCCCCACTCAATGCACTCCATG, the mutation M38A (the hypothetical translation reinitiation methionine) using the primers P-CCTCTGGGGAAGCCAGCCGCGCTGCACCTGCCTTCAGAAC and P-GTTCTGAAGGCAGGTGCAGCGCGGCTGGCTTCCCCAGAGG, the double mutation *110_111insC*/M38A using the primers P-CCTCTGGGGAAGCCAGCCCGCGCTGCACCTGCCTTCAGAAC and P-GTTCTGAAGGCAGGTGCAGCGCGGGCTGGCTTCCCCAGAGG, and the mutation M94A (the second hypothetical translation reinitiation methionine) using the primers P-GAGGAGAAGGAGTTCCTCGCGTGCAAGTTCCAGGAGGCC and P-GGCCTCCT-

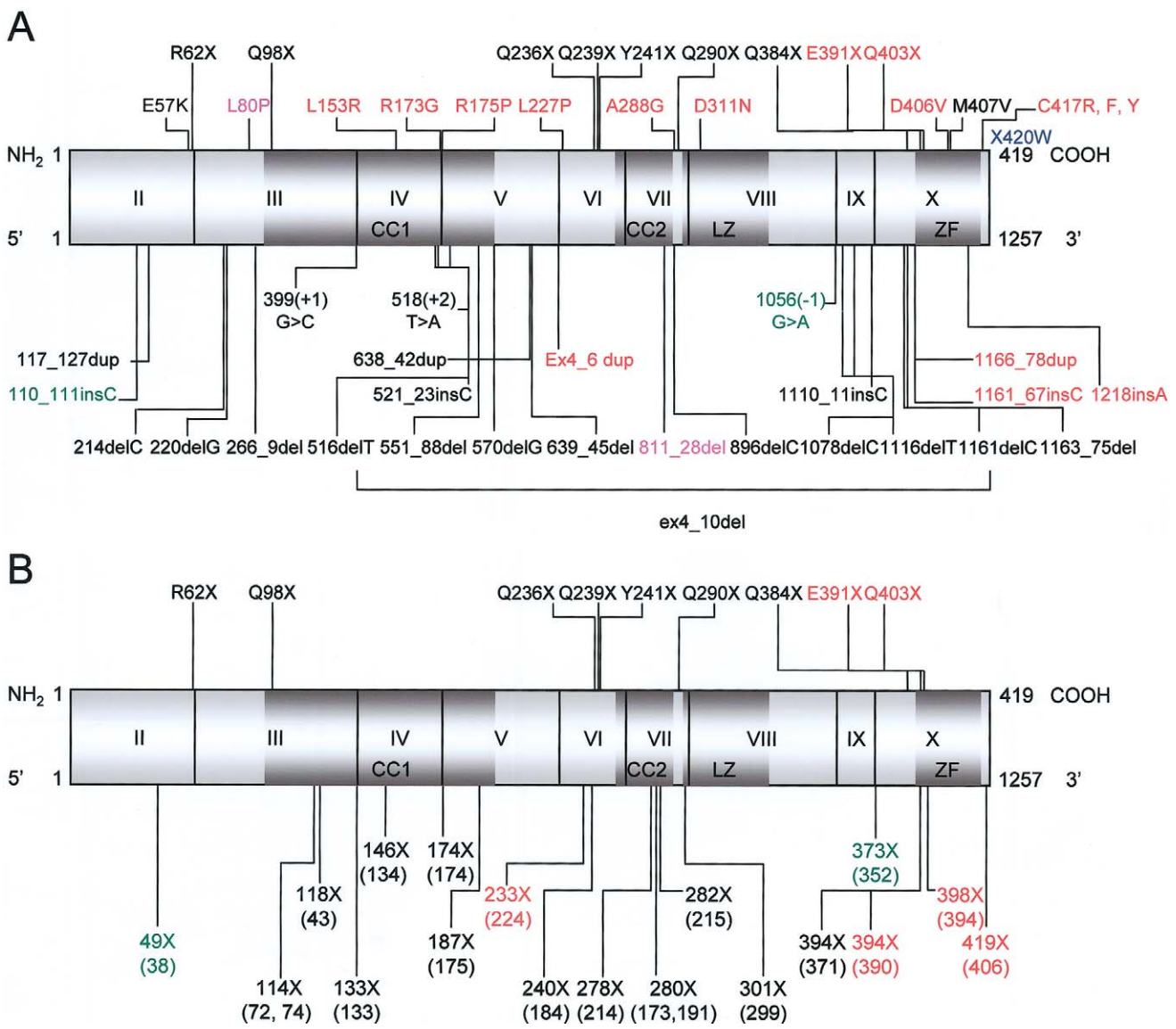

Figure 2 Schematic representation of *NEMO* with all reported mutations. *A,* Schematic representation of the coding-region domain organization: coil-coiled (CC), leucine-zipper (LZ), and zinc-finger (ZF) domains, and published mutations of *NEMO*. *B,* Schematic representation of all known premature stop codons in *NEMO* due to nonsense and splice mutations, frameshift insertions, and deletions. For the mutations leading to a frameshift, the position of the premature stop codon is indicated, with the position of the first amino acid affected by the mutation in parentheses. The mutations associated with XD-IP are shown in black, with XR-OL-EDA-ID in blue, with XR-EDA-ID without OL in red, with incomplete XR-I-EDA-ID in pink, and with XR-ID without EDA in green.

GGAACTTGCACGCGAGGAACTCCTTCTCCTC. The mutated fragments were then subcloned into the pcDNA3.1/V5-*His*-directional TOPO expression vector (Invitrogen SARL), in accordance with the manufacturer's instructions.

The various pcDNA3.1/V5-His-TOPO expression vectors encoding wild-type (WT), *110_111insC, 110_111insC*/M38A, M38A, M94A, R62X, and X420W NEMO or the insert-free vector were used to transfect SV40-transformed IP fibroblasts or 293T HEK cells, in the presence of Lipofectamine 2000 (Invitrogen SARL) or calcium phosphate (Invitrogen SARL), in accordance with the manufacturer's recommendations.

For intracellular NEMO staining, we fixed 2×10^5 fibroblasts or EBV-transformed B cells, permeabilized them using IntraStain kit (DakoCytomation S.A.S. Trappes Cedex), and incubated them with a mouse anti-human IKKγ/NEMO IgG1 (611306) from BD Transduction Laboratories (Becton Dickinson France S.A.S.) or an isotype control mouse IgG1,κ, (555746) from BD

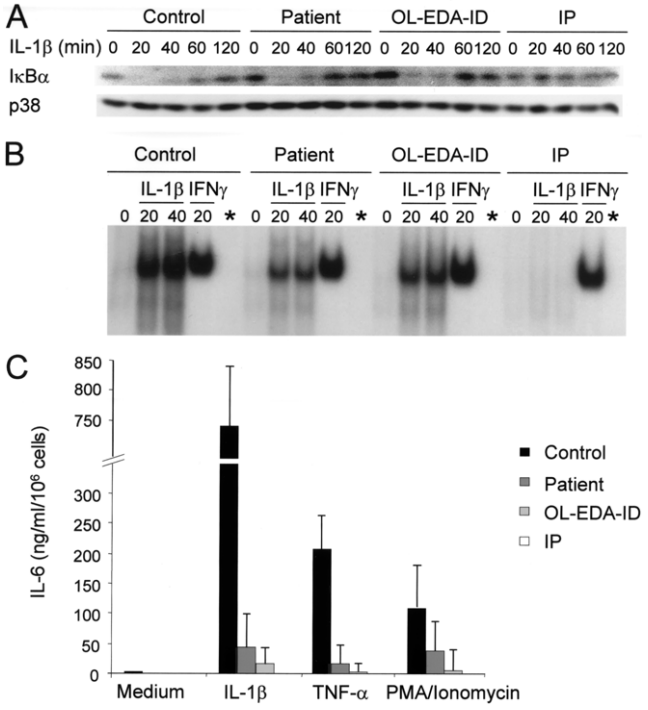

Figure 3 NF-κB signaling in SV40-transformed fibroblasts. *A,* Time-course analysis of IκBα protein degradation and resynthesis detected by western blot after stimulation with IL-1β for 20, 40, 60, and 120 min; the antibody against p38 served as a control for protein loading. *B,* NF-κB DNA-binding activity, measured by EMSA after stimulation for 20 and 40 min with IL-1β. γ-Activating–factor DNA-binding activity after 20 min of stimulation with IFN-γ and competition with unlabeled NF-κB–specific probe (*) served as internal activation control and specificity control, respectively. *C,* IL-6 production after 18 h of exposure to IL-1β, TNF-α, and PMA/ionomycin, in fibroblasts from a healthy control, from the patient, from a patient with XR-OL-EDA-ID (X420W), and from a patient with XD-IP (*ex4_10del*). Results shown are representative of two to three independent experiments.

Pharmingen (Becton Dickinson France S.A.S.). Cells were washed and were labeled with an Alexa Fluor 488 goat anti-mouse IgG (A-11029) from Molecular Probes (Invitrogen SARL), as described elsewhere (Nishikomori et al. 2004). Cells were analyzed by flow cytometry on a FACScan apparatus (Becton Dickinson).

The sequencing of genomic DNA and cDNA obtained from whole blood cells, granulocytes, SV40-transformed fibroblasts, and EBV-transformed B cells revealed a frameshift insertion in codon 37 of *NEMO* exon 2 (*110_111insC*) generating a premature stop codon 12 residues downstream at codon position 49 (*M38fsX48*) (figs. 1*A,* 2*A,* and 2*B*). The mother, maternal aunt, and maternal grandmother of this patient were heterozygous for the mutation (fig. 1*B*). This previously unreported mutation was not found in 305 Caucasian controls (190 females and 115 males; 495 chromosomes), suggesting that it was pathogenic. It creates the furthest upstream of the known premature stop codons in *NEMO*—most others being associated with XD-IP, and the remaining few, mostly located in the 3′ region of the coding region, being associated with XR-EDA-ID (fig. 2*A* and 2*B*). Paradoxically, the *110_111insC* mutation was associated with viable fetal development and a lack of detectable developmental phenotype in the affected hemizygous boy. Moreover, the mother presented no clinical signs of XD-IP and displayed a random pattern of X-chromosome inactivation (75% and 25%) in her blood cells (fig. 1*C*).

We investigated whether the *110_111insC* mutation was amorphic (as in loss-of-function), as predicted from genetic findings, or hypomorphic, as predicted from clinical findings, by assessing NF-κB activation in SV40-transformed fibroblasts from a healthy control, from the patient studied, from a patient with XR-OL-EDA-ID (bearing the NEMO X420W mutation), and from a fetus with XD-IP (bearing the *ex4-10del NEMO* mutation). Upon stimulation with TNF-α and IL-1β, IκBα degradation and resynthesis were normal in the patient's cells, whereas they were impaired in XR-OL-EDA-ID cells and were completely abolished in XD-IP cells (fig. 3*A* and data not shown). However, the κB DNA-binding activity of the patient's cells, measured by EMSA, was approximately one-third that of control fibroblasts—a decrease similar to that observed with XR-OL-EDA-ID fibroblasts. No detectable DNA-binding activity was observed with XD-IP fibroblasts (figs. 3*B* and 4). Finally, IL-6 production was impaired in the patient's fibroblasts and, to a greater extent, in XR-OL-EDA-ID fibroblasts, in response to both IL-1β and TNF-α, whereas it was completely abolished in XD-IP fibroblasts (fig. 3*C*). Thus, the *NEMO 110_111insC* mutation, despite creating a stop codon at position 49, was hypomorphic, since it impaired but did not abolish NF-κB activation and was even associated with a somewhat milder cellular phenotype than the X420W *NEMO* mutation.

We evaluated the immunological impact of the *NEMO* mutation by stimulating the patient's blood cells (fig. 5) with TNF-α, IL-1β, or agonists of TLRs. The response of the patient's blood cells to TNF-α was reproducibly impaired, in terms of IL-10 production. In contrast, the response to IL-1β, LPS (an agonist of TLR-4), or other TLR agonists—such as heat-killed *S. aureus* Cowan, *E. coli,* and *M. tb*—was normal, in terms of IL-6 or TNF-α production. Because the main infectious disease of this patient was caused by *M. avium,* a weakly virulent environmental mycobacterial species, we also investigated the IL-12/23-IFN-γ circuit (Casanova and Abel 2002). We observed no response to live *M. bovis* BCG, BCG plus IL-12, or BCG plus IFN-γ, in terms of IFN-γ, IL-12p40, or IL-12p70 production in the patient's blood cells. Finally, we tested CD40-mediated

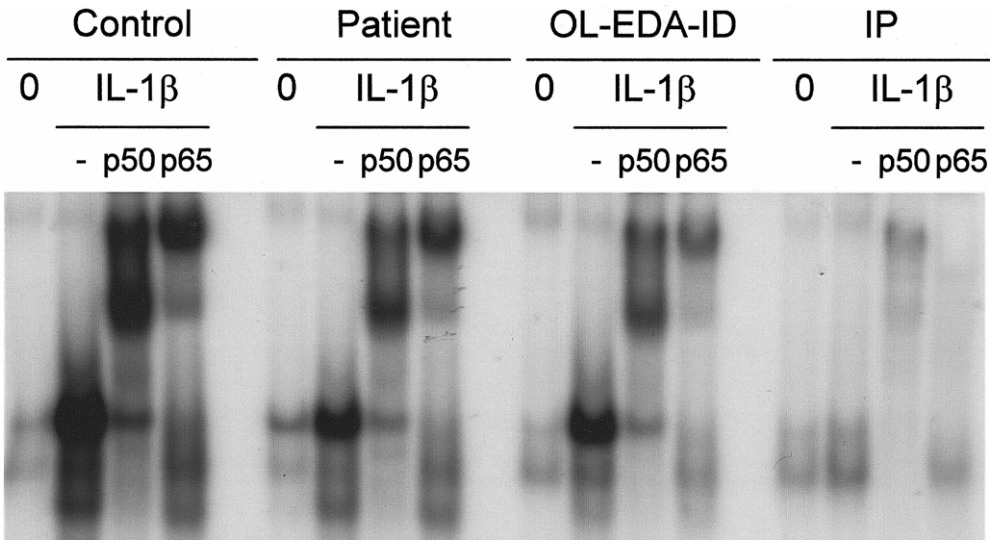

Figure 4 NF-κB signaling in fibroblasts. Composition of the NF-κB dimers bound to the κB probe, as measured by EMSA in SV40-transformed fibroblasts from a healthy control, from the patient, from a patient with OL-EDA-ID, and from a patient with IP, after exposure to IL-1β for 40 min, and as determined using antibodies directed against p50 and p65.

NF-κB activation by measuring B-cell proliferation and Ig isotype switching upon stimulation with CD40L (CD154) in vitro. The patient's cells displayed impaired proliferation and IgE production in response to CD154, alone or in combination with IL-4. These results indicate that the patient's *NEMO* mutation was hypomorphic in blood cells and provide an explanation for the patient's immunological phenotype.

We then assessed NEMO production in SV40-transformed fibroblasts from the patient. No protein was detected in the patient's fibroblasts with the use of a serum directed against N-terminal amino acids 28–33 of NEMO (serum 3328), whereas two proteins of ~48 and 45 kDa were detected in control cells (fig. 6*A*, left panel), and a protein of ~51 kDa appeared with prolonged exposure in the OL-EDA-ID fibroblasts (data not shown). In contrast, with the use of antibodies directed against amino acids 278–396 (611306) (data not shown) and 356–414 (M-18) (fig. 6*A*, right panel), small amounts of a protein of ~45 kDa were detected in the control and patient's fibroblasts. Neither the 48-kDa nor the 45-kDa protein was detected with either antibody in XD-IP fibroblasts, suggesting that the *NEMO* gene encoded both proteins. Residual NEMO production was detected by flow cytometry, with use of antibody 611306 in fibroblasts (fig. 6*B*) and EBV-transformed B cells (not shown) from the patient and from the patient with XR-OL-EDA-ID. Again, no NEMO was detected in XD-IP fibroblasts. Thus, the *110_111insC* mutant allele encodes an N-terminally truncated NEMO protein that is produced in small amounts. The *110_111insC* mutation probably allows reinitiation of the translation process downstream from the insertion.

An almost canonically Kozakian methionine AUG start codon (Kozak 2000, 2002*b*) is located at nucleotide positions 112–114, corresponding to methionine 38 (fig. 7*A*). The likelihood of this AUG codon acting as a translation initiation site was estimated at 0.27 and increased to 0.51 in the sequence context found in the patient, versus 0.63 for the first AUG codon (Prediction of Translation Initiation ATG Web site). Such a reinitiation of translation would result in the synthesis of a protein ~45 kDa in size. We, therefore, transfected 293T HEK cells with V5-tagged expression vectors carrying WT and various mutant *NEMO* alleles: M38A (methionine 38 replaced by alanine, preventing reinitiation at codon 38) with or without the *110_111insC,* R62X (the most-upstream nonsense mutation responsible for XD-IP), and X420W. With an anti-V5 antibody, a protein of ~48 kDa was detected in WT- and M38A-transfected cells. Smaller amounts of a protein of ~45 kDa were detected

The figure is available in its entirety in the online edition of *The American Journal of Human Genetics.*

Figure 5 Whole blood cell activation. The legend is available in its entirety in the online edition of *The American Journal of Human Genetics.*

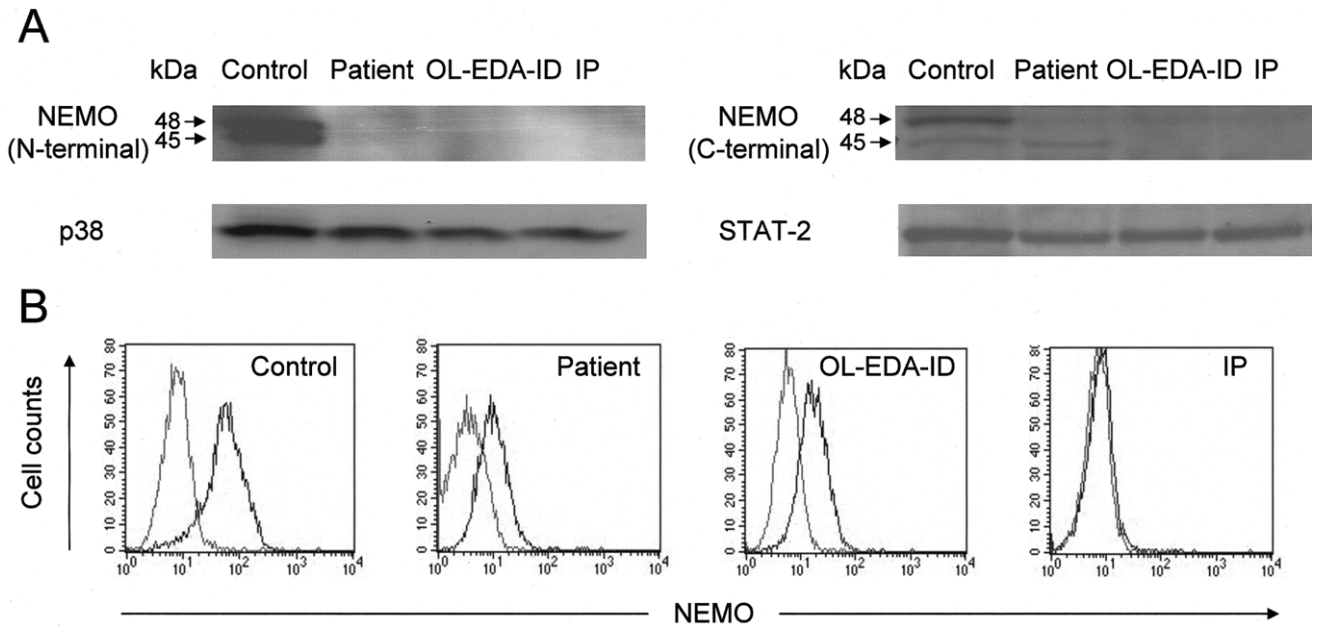

Figure 6 NEMO production in SV40-transformed fibroblasts. *A,* NEMO production assessed by western blot analysis, with the use of antibodies directed against the N- or C-terminal part of NEMO (amino acids 28–33 and 356–414, respectively), antibodies against p38 and STAT-2 being used as controls for protein loading. *B,* Intracellular staining with an antibody directed against amino acids 278–396 of NEMO (*black*) or an isotype-control antibody (*gray*) of fibroblasts from a control, from the patient, from a patient with XR-OL-EDA-ID, and from a patient with XD-IP. Results shown are representative of three independent experiments.

in WT- and *110_111insC*-transfected cells, but not in M38A- or *110_111insC*/M38A–transfected cells. A protein of ~51 kDa was detected in X420W-transfected cells, and no specific proteins were detected in mock- and *NEMO* R62X-transfected cells. These results confirmed that the WT *NEMO* allele encodes two proteins: the predominant 48-kDa protein and an N-terminally truncated protein of ~45 kDa produced in smaller amounts and translated from methionine 38. This second protein is the only isoform detected in the patient's cells.

This description of the most-upstream premature stop codon (at amino-acid position 49, *M38fsX48*) of any known *NEMO* mutation, in a child with ID without EDA, shows that the location of the premature stop codon is not correlated with the severity of the clinical phenotype. Nonetheless, the ID appeared to be particularly severe, since the patient developed fatal HSV-1 meningo-encephalitis (Niehues et al. 2004), identifying NEMO deficiency as the second genetic etiology of HSV-1 encephalitis (Dupuis et al. 2003) and suggesting that the NF-κB–mediated induction of IFN-α/β is essential for HSV-1 control. The *110_111insC* mutation, therefore, had a highly deleterious effect on immunity to infection but a much weaker than expected effect on development, with normal fetal development and no signs of EDA in childhood. Studies on the patient's cells showed that the *110_111insC NEMO* mutation was hypomorphic because of the residual production of an N-terminally truncated protein resulting from the reinitiation of translation at an internal AUG codon located immediately downstream from the mutation. This process also occurs in control cells. The small amounts of the resulting NEMO protein were sufficient to trigger normal responses to some NF-κB dependent signaling pathways, preventing both fetal death and developmental disorders in childhood (Smahi et al. 2002).

This rare mechanism has been reported in other inherited disorders of leukocytes—such as Omenn's syndrome (*RAG1*) (Santagata et al. 2000), Fanconi anemia (*FAC*) (Yamashita et al. 1996), and Nijmegen breakage syndrome (*NBS1*) (Maser et al. 2001)—and in other fields of human genetics (Yamashita et al. 1996; Ozisik et al. 2003; Pittis et al. 2004), upstream premature stop codons being typically involved (Santagata et al. 2000). Nevertheless, this compensatory mechanism is only partial, because (1) reinitiation at a secondary AUG is less efficient than use of the first AUG (Kozak 2002*a*), (2) truncated proteins are potentially unstable, and (3) truncated proteins are likely to be less functional. There is currently no documented example of full biological or clinical complementation of a premature stop codon by

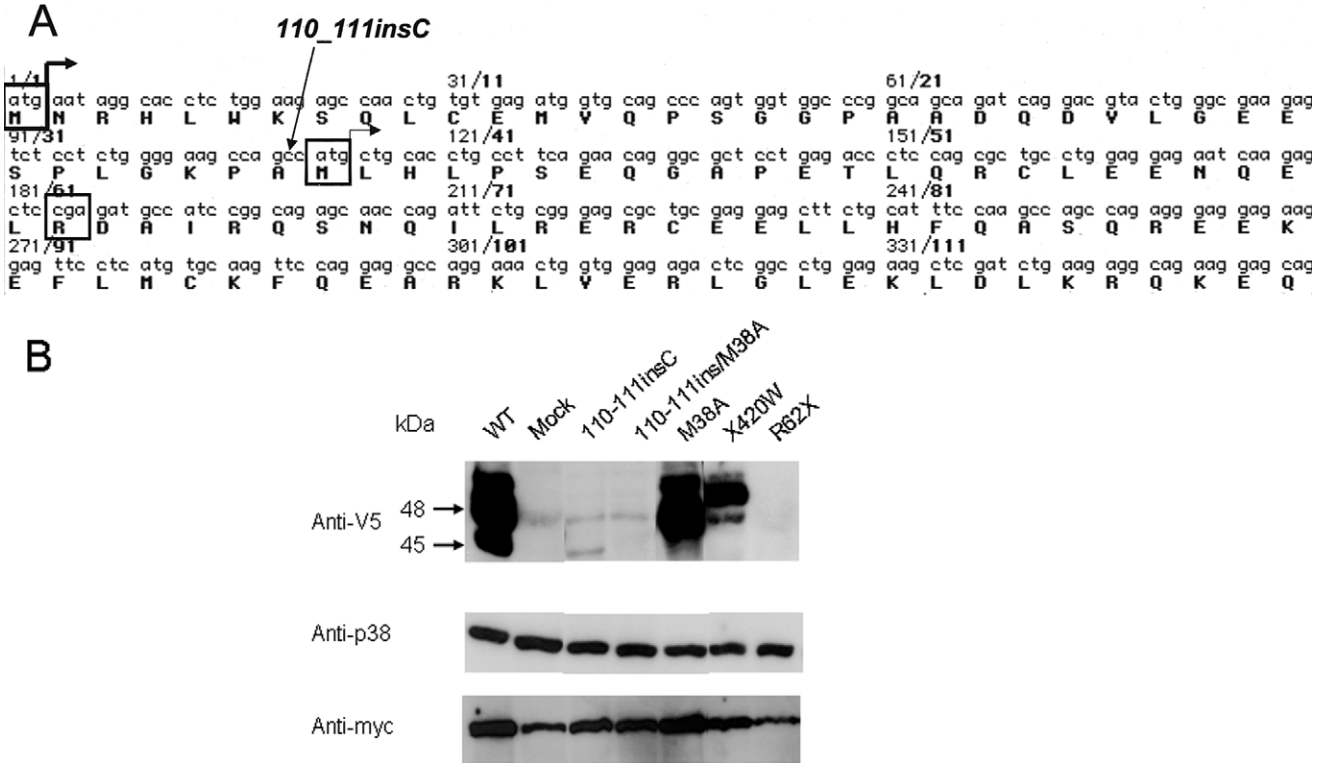

Figure 7 Expression of various *NEMO* constructs in vitro. *A*, WT sequence of the 5′ end of *NEMO* showing the first methionine site involved in the initiation of translation (M1, *boxed*), the position of the *110_111insC* mutation, the second methionine site (M38) involved in translation reinitiation, and the IP nonsense mutation at Arg 62 (R62X). *B*, Western blot analysis with an anti-V5 antibody of 293T HEK cells transfected with insert-free V5-tagged vector (mock) or with expression vectors carrying various *NEMO* alleles: WT, *110_111insC* (the patient's mutation), M38A (the methionine 38 to alanine mutation, blocking reinitiation of translation at M38) with or without the *110_111insC* mutation, X420W, and R62X. Cells were cotransfected with 3 μg of each vector and 1 μg of a myc-tagged expression vector encoding β-galactosidase, as a transfection-efficiency control. An antibody against p38 was used to control for protein loading.

reinitiation of translation. However, some compensation does occur, the cellular and clinical phenotypes being milder than predicted from the genotype alone (Yamashita et al. 1996; Santagata et al. 2000; Maser et al. 2001). This report therefore adds a further level of complexity to studies of pathogenic mutations in human *NEMO* and provides further evidence that the reinitiation of translation is a potentially important compensatory mechanism in human genetics, with profound cellular and clinical consequences.

Acknowledgments

This work was supported in part by grants from the Institut Universitaire de France and the Schlumberger and BNP-Paribas Foundations. Anne Puel was supported by a European grant (QLK2-CT-2002-00846), and Janine Reichenbach was supported by the Lise Meitner program. We thank the patient and his family for their willingness to participate in this study, and we thank the numerous clinicians and scientists who collaborated with us. We thank Tony Leclerc, for expert technical assistance; Arnold Munnich, Laurent Abel, and all members of the Laboratory of Human Genetics of Infectious Diseases, for helpful discussions; Adrian Ozinsky (University of Washington), Richard Miller (3M Pharmaceuticals), and Franck Barrat (Dynavax), for helpful discussions and for the TLR agonists; and Sandra Weller, for B-cell subpopulation studies. Jean-Laurent Casanova is an International Scholar of the Howard Hughes Medical Institute.

Web Resources

The URL for data presented herein is as follows:

Prediction of Translation Initiation ATG, http://www.hri.co.jp/atgpr/

References

Abinun M, Spickett G, Appleton AL, Flood T, Cant AJ (1996) Anhidrotic ectodermal dysplasia associated with specific antibody deficiency. Eur J Pediatr 155:146–147

Allen RC, Zoghbi HY, Moseley AB, Rosenblatt HM, Belmont JW (1992) Methylation of *Hpa*II and *Hha*I sites near the polymorphic

CAG repeat in the human androgen-receptor gene correlates with X chromosome inactivation. Am J Hum Genet 51:1229–1239

Aradhya S, Courtois G, Rajkovic A, Lewis RA, Levy M, Israel A, Nelson DL (2001*a*) Atypical forms of incontinentia pigmenti in male individuals result from mutations of a cytosine tract in exon 10 of NEMO (IKK-gamma). Am J Hum Genet 68:765–771

Aradhya S, Woffendin H, Jakins T, Bardaro T, Esposito T, Smahi A, Shaw C, Levy M, Munnich A, D'Urso M, Lewis RA, Kenwrick S, Nelson DL (2001*b*) A recurrent deletion in the ubiquitously expressed NEMO (IKK-gamma) gene accounts for the vast majority of incontinentia pigmenti mutations. Hum Mol Genet 10:2171–2179

Carrol ED, Gennery AR, Flood TJ, Spickett GP, Abinun M (2003) Anhidrotic ectodermal dysplasia and immunodeficiency: the role of NEMO. Arch Dis Child 88:340–341

Casanova JL, Abel L (2002) Genetic dissection of immunity to mycobacteria: the human model. Annu Rev Immunol 20:581–620

Chitnis S, Monteiro J, Glass D, Apatoff B, Salmon J, Concannon P, Gregersen PK (2000) The role of X-chromosome inactivation in female predisposition to autoimmunity. Arthritis Res 2:399–406

Döffinger R, Smahi A, Bessia C, Geissmann F, Feinberg J, Durandy A, Bodemer C, et al (2001) X-linked anhidrotic ectodermal dysplasia with immunodeficiency is caused by impaired NF-kappaB signaling. Nat Genet 27:277–285

Dupuis S, Jouanguy E, Al-Hajjar S, Fieschi C, Al-Mohsen IZ, Al-Jumaah S, Yang K, Chapgier A, Eidenschenk C, Eid P, Al Ghonaium A, Tufenkeji H, Frayha H, Al-Gazlan S, Al-Rayes H, Schreiber RD, Gresser I, Casanova JL (2003) Impaired response to interferon-alpha/beta and lethal viral disease in human STAT1 deficiency. Nat Genet 33:388–391

Dupuis-Girod S, Corradini N, Hadj-Rabia S, Fournet JC, Faivre L, Le Deist F, Durand P, Döffinger R, Smahi A, Israel A, Courtois G, Brousse N, Blanche S, Munnich A, Fischer A, Casanova JL, Bodemer C (2002) Osteopetrosis, lymphedema, anhidrotic ectodermal dysplasia, and immunodeficiency in a boy and incontinentia pigmenti in his mother. Pediatrics 109:e97

Fusco F, Bardaro T, Fimiani G, Mercadante V, Miano MG, Falco G, Israel A, Courtois G, D'Urso M, Ursini MV (2004) Molecular analysis of the genetic defect in a large cohort of IP patients and identification of novel NEMO mutations interfering with NF-kappaB activation. Hum Mol Genet 13:1763–1773

Jain A, Ma CA, Liu S, Brown M, Cohen J, Strober W (2001) Specific missense mutations in NEMO result in hyper-IgM syndrome with hypohydrotic ectodermal dysplasia. Nat Immunol 2:223–228

Jain A, Ma CA, Lopez-Granados E, Means G, Brady W, Orange JS, Liu S, Holland S, Derry JM (2004) Specific NEMO mutations impair CD40-mediated c-Rel activation and B cell terminal differentiation. J Clin Invest 114:1593–1602

Kosaki K, Shimasaki N, Fukushima H, Hara M, Ogata T, Matsuo N (2001) Female patient showing hypohidrotic ectodermal dysplasia and immunodeficiency (HED-ID). Am J Hum Genet 69:664–666

Kozak M (2000) Do the 5′ untranslated domains of human cDNAs challenge the rules for initiation of translation (or is it vice versa)? Genomics 70:396–406

——— (2002*a*) Emerging links between initiation of translation and human diseases. Mamm Genome 13:401–410

——— (2002*b*) Pushing the limits of the scanning mechanism for initiation of translation. Gene 299:1–34

Ku CL, Dupuis-Girod S, Dittrich AM, Bustamante J, Santos OF, Schulze I, Bertrand Y, Couly G, Bodemer C, Bossuyt X, Picard C, Casanova JL (2005*a*) NEMO mutations in 2 unrelated boys with severe infections and conical teeth. Pediatrics 115:e615–e619

Ku CL, Yang K, Bustamante J, Puel A, von Bernuth H, Santos OF, Lawrence T, Chang HH, Al-Mousa H, Picard C, Casanova JL (2005*b*) Inherited disorders of human Toll-like receptor signaling: immunological implications. Immunol Rev 203:10–20

Mansour S, Woffendin H, Mitton S, Jeffery I, Jakins T, Kenwrick S, Murday VA (2001) Incontinentia pigmenti in a surviving male is accompanied by hypohidrotic ectodermal dysplasia and recurrent infection. Am J Med Genet 99:172–177

Maser RS, Zinkel R, Petrini JH (2001) An alternative mode of translation permits production of a variant NBS1 protein from the common Nijmegen breakage syndrome allele. Nat Genet 27:417–421

Niehues T, Reichenbach J, Neubert J, Gudowius S, Puel A, Horneff G, Lainka E, Dirksen U, Schroten H, Döffinger R, Casanova JL, Wahn V (2004) Nuclear factor kappaB essential modulator-deficient child with immunodeficiency yet without anhidrotic ectodermal dysplasia. J Allergy Clin Immunol 114:1456–1462

Nishikomori R, Akutagawa H, Maruyama K, Nakata-Hizume M, Ohmori K, Mizuno K, Yachie A, Yasumi T, Kusunoki T, Heike T, Nakahata T (2004) X-linked ectodermal dysplasia and immunodeficiency caused by reversion mosaicism of NEMO reveals a critical role for NEMO in human T-cell development and/or survival. Blood 103:4565–4572

Orange JS, Brodeur SR, Jain A, Bonilla FA, Schneider LC, Kretschmer R, Nurko S, Rasmussen WL, Kohler JR, Gellis SE, Ferguson BM, Strominger JL, Zonana J, Ramesh N, Ballas ZK, Geha RS (2002) Deficient natural killer cell cytotoxicity in patients with IKK-gamma/NEMO mutations. J Clin Invest 109:1501–1509

Orange JS, Jain A, Ballas ZK, Schneider LC, Geha RS, Bonilla FA (2004*a*) The presentation and natural history of immunodeficiency caused by nuclear factor kappaB essential modulator mutation. J Allergy Clin Immunol 113:725–733

Orange JS, Levy O, Brodeur SR, Krzewski K, Roy RM, Niemela JE, Fleisher TA, Bonilla FA, Geha RS (2004*b*) Human nuclear factor kappa B essential modulator mutation can result in immunodeficiency without ectodermal dysplasia. J Allergy Clin Immunol 114:650–656

Ozisik G, Mantovani G, Achermann JC, Persani L, Spada A, Weiss J, Beck-Peccoz P, Jameson JL (2003) An alternate translation initiation site circumvents an amino-terminal DAX1 nonsense mutation leading to a mild form of X-linked adrenal hypoplasia congenita. J Clin Endocrinol Metab 88:417–423

Parrish JE, Scheuerle AE, Lewis RA, Levy ML, Nelson DL (1996) Selection against mutant alleles in blood leukocytes is a consistent feature in Incontinentia Pigmenti type 2. Hum Mol Genet 5:1777–1783

Picard C, Puel A, Bonnet M, Ku CL, Bustamante J, Yang K, Soudais C, et al (2003) Pyogenic bacterial infections in humans with IRAK-4 deficiency. Science 299:2076–2079

Pittis MG, Ricci V, Guerci VI, Marcais C, Ciana G, Dardis A, Gerin F, Stroppiano M, Vanier MT, Filocamo M, Bembi B (2004) Acid sphingomyelinase: identification of nine novel mutations among Italian Niemann Pick type B patients and characterization of in vivo functional in-frame start codon. Hum Mutat 24:186–187

Priolo M, Lagana C (2001) Ectodermal dysplasias: a new clinical-genetic classification. J Med Genet 38:579–585

Puel A, Picard C, Ku CL, Smahi A, Casanova JL (2004) Inherited disorders of NF-kappaB-mediated immunity in man. Curr Opin Immunol 16:34–41

Santagata S, Gomez CA, Sobacchi C, Bozzi F, Abinun M, Pasic S, Cortes P, Vezzoni P, Villa A (2000) N-terminal RAG1 frameshift mutations in Omenn's syndrome: internal methionine usage leads to partial V(D)J recombination activity and reveals a fundamental role in vivo for the N-terminal domains. Proc Natl Acad Sci USA 97:14572–14577

Smahi A, Courtois G, Rabia SH, Döffinger R, Bodemer C, Munnich A, Casanova JL, Israel A (2002) The NF-kappaB signalling pathway in human diseases: from incontinentia pigmenti to ectodermal dys-

plasias and immune-deficiency syndromes. Hum Mol Genet 11: 2371–2375

Smahi A, Courtois G, Vabres P, Yamaoka S, Heuertz S, Munnich A, Israel A, et al (2000) Genomic rearrangement in NEMO impairs NF-kappaB activation and is a cause of incontinentia pigmenti: the International Incontinentia Pigmenti (IP) Consortium. Nature 405: 466–472

Yamashita T, Wu N, Kupfer G, Corless C, Joenje H, Grompe M, D'Andrea AD (1996) Clinical variability of Fanconi anemia (type C) results from expression of an amino terminal truncated Fanconi anemia complementation group C polypeptide with partial activity. Blood 87:4424–4432

Zonana J, Elder ME, Schneider LC, Orlow SJ, Moss C, Golabi M, Shapira SK, Farndon PA, Wara DW, Emmal SA, Ferguson BM (2000) A novel X-linked disorder of immune deficiency and hypohidrotic ectodermal dysplasia is allelic to incontinentia pigmenti and due to mutations in IKK-gamma (NEMO). Am J Hum Genet 67: 1555–1562